

Phosphorrückgewinnung aus industriellen und kommunalen Abwässern mittels eines Fließbettreaktors

Pengfei Wang und Carsten Meyer

Institut für Siedlungswasserbau, Wassergüte- und Abfallwirtschaft, Universität Stuttgart

Abstract

Within the last decades shifting from phosphorus (P) removal to P recovery in wastewater treatment plants (WWTPs) has been a new trend. Struvite ($\text{MgNH}_4\text{PO}_4 \cdot 6\text{H}_2\text{O}$) crystallization is a promising P recovery technology because the recovered struvite is a functional slow release fertilizer. The fluidized bed reactor (FBR) is the most studied type of reactor for struvite crystallization. However, there is a lack of consensus about the reactor design and its operation; the formation process of the large compact struvite particles in the FBR remains a black box, and struvite crystallization FBR has not been integrated yet in WWTPs with chemical P removal. In this study, two lab-scale FBRs were constructed and several continuous struvite crystallization experiments with synthetic wastewater and three types of real wastewater were carried out with them. The results revealed that pH played a decisive role in the process efficiency while all of the pH, hydraulic retention time, seed size, recirculation flow rate and the experiment duration influenced the size, morphology and compactness of the produced struvite particles. The struvite particles grown from small struvite seeds broke in the reactor during the experiment with the adjusted sludge filtrate from the Treatment Plant for Education and Research of the University of Stuttgart (LFKW). 2-4 mm compact spherical struvite particles were successively produced in the experiments with the industrial wastewater from the dairy company Campina AG Heilbronn and the pre-treated sludge filtrate from the Offenburg WWTP with chemical P removal when large struvite particles were added as seeds. These compact particles were composed of inner cores of the seed crystal aggregates and outer compact small-crystal layers. The purity of the produced struvite particles from all of the three real wastewaters was higher than 95%. However, their mass percentage among the entire harvested product was very small, in which further research is needed.

1 Introduction

In order to prevent eutrophication, phosphorus (P) removal has been integrated in wastewater treatment plants (WWTPs) in Europe since the middle to late 20th century (Günther, 1996). Two P removal methods are generally used: chemical precipitation and enhanced biological P removal (EBPR). Both of them transfer the P from the wastewater into the sewage sludge. Within the last decades shifting from P removal to P recovery in WWTP has been a new trend, because the quality of phosphate rock which is the predominant source of P is deteriorating with a decreasing grade and increasing heavy metal contents (Cordell et al., 2009), and wastewater tends to be a substantial alternative P source. Globally, humans excrete about 3 million metric tons (Mt) of P into the wastewater each year (Cordell et al., 2009). If all the P was recovered and used as fertilizer, it would compensate the global

P fertilizer consumption which added up to 40.3 Mt P₂O₅ in 2012/13 (Heffer and Prud'homme, 2013) by 17%.

Struvite (MgNH₄PO₄·6H₂O) crystallization is a promising P recovery technology because the recovered struvite is a functional slow release fertilizer with low heavy metal contents and a long fertilizing effect. Struvite crystallization is based on the equation:



with the value of n equal to 0, 1 or 2 depending on the operation pH. Moreover, struvite crystallization is influenced by a number of factors, including the thermodynamics and kinetics of reactions, mass transfer between solid and liquid phases as well as several physico-chemical parameters: pH, supersaturation level, mixing energy, temperature and the presence of foreign ions (Le Corre et al., 2009). The fluidized bed reactor (FBR) is the most studied type of reactor for struvite crystallization (Le Corre et al., 2009). However, there is a lack of consensus about the reactor design and operation. For example, based on practical experiences, Fattah (2010) stated that there was an upper limit of upflow velocity (400 cm/min) at which a struvite crystallization FBR should be operated at, in order to produce good quality pellets. Higher upflow velocity (500 cm/min) destroyed the shape and reduced the strength of the product. Nevertheless, Piekema and Giesen (2001) reported a much lower empirical appropriate upflow velocity range of 67-125 cm/min. Moreover, the formation process of the large compact struvite particles in the FBR was never reported and remains a black box. The literature suggests that almost all of the struvite crystallization FBRs were operated with digested sludge supernatant or centrate from the WWTPs using EBPR, and this type of reactor has not been integrated in WWTPs with chemical P removal. Since in Germany a large part of WWTPs (61% based on population equivalent, 43% based on WWTP amount) use mainly chemical P removal (DWA, 2005 in Montag, 2008), and a P concentration of 1000 mg/L can be reached after appropriate pre-treatment of such sludge (Weideler, 2010), it seems to make sense to recover the P from WWTPs with chemical P removal using the struvite crystallization FBR.

The main aims of this project are to understand the formation process of the compact struvite particles in the FBR, to clarify the influences of several operational parameters on the process efficiency and the product quality by conducting continuous struvite crystallization experiments with synthetic wastewater, and to recover P as large compact struvite particles from the industrial wastewater and pre-treated sludge filtrate from the WWTP with chemical P removal with the struvite crystallization FBR.

2 Materials and methods

2.1 Experimental setup

Two lab-scale FBRs: the old and the new reactor were constructed with transparent polyvinyl chloride (PVC) tubes in this study. Figure 1 (left) shows a schematic of the experimental setup with the old FBR. The reactor consisted of a reaction section and a precipitation section. The diameter of the precipitation was 13.6 cm. The large diameter enabled a small velocity in the precipitation section so that the small crystals could settle. The main part of

The pH of the in-reactor solution was measured with a pH electrode (SenTix®, WTW, Germany) and a pH meter (WTW, Germany). With the old reactor, the pH electrode was located in the 4.2 cm reaction section. With the new reactor, it was located on the top of the reactor so that it could be taken out and calibrated during the experiment. The pH meter was connected to a computer. With a pH controlling software, VMP UmweltLabor V1.0 developed by Volker Preyl of ISWA, the measured pH data was recorded once every 30 s and the pH of the in-reactor solution was maintained at a certain value by controlling the on and off of the NaOH dosing pump. Harvesting of the in-reactor particles was accomplished by collecting a product collector filled with the effluent solution to the FBR with a rubber pipe. By reducing the recirculation flow rate, the large particles which could overcome the upflow velocity of the bottom section fell into the collector. After closing the rubber pipe with a clamp, the particles were discharged from the collector and were harvested.

2.2 Reactor operation and measurements

During each continuous experiment, the wastewater tank, Mg solution tank and the NaOH solution bottle were refilled every 1 or 2 d. The effluent during each 24 h was collected with a tank and the 24 h composite effluent sample was taken. The phosphate-phosphorus ($\text{PO}_4\text{-P}$) and ammonium-nitrogen ($\text{NH}_4\text{-N}$) concentrations of the feed wastewater and the 24 h composite effluent were measured daily with spectrophotometry after filtration with the 0.45 μm membrane filters. In the experiments with real wastewater, the metal ion (Al, Ca, Fe and Mg) concentrations were measured additionally by ICP-OES. The Mg concentration of the Mg solution was measured every time after refilling by titration with the ethylenediaminetetraacetic acid (EDTA) solution. On the days when a lot fine crystals were generated and flushed out of the reactor with the effluent, which was referred as the fines problem, the total phosphorus (TP) concentration of the effluent was also measured. The daily NaOH solution consumption amount was determined by weighing the NaOH solution bottle at the beginning and the end of each 24 h during which the effluent was collected.

After every 7 days' continuous operation, some of the largest in-reactor particles were harvested; at the end of the experiment, all of the in-reactor crystals and particles were harvested. The harvested crystals and particles were left on the paper filter and dried at room temperature for at least 7 d. Then they were dried with flowing warm air at 30°C for 48 h when constant weight was reached. The size of the dried crystals and particles were measured by sieving with the test sieves (DIN 4188 type, Retsch, Germany) with mesh sizes of 0.020, 0.045, 0.125, 0.250, 0.355, 0.560, 0.710, 0.8, 1.0, 1.4, 2.0, 2.5, 2.8 and 3.15 mm. The size of the larger than 3.15 mm particles was measured with a micrometer. The TP and total Kjeldahl nitrogen (TKN) contents of the particles were measured after grinding. In the experiments with real wastewater, the metal ion contents of the particles were also measured with ICP-OES. The particles were examined with an x-ray diffractometer (D8 Advance, Bruker AXS, Germany) to determine the crystalline composition and their morphologies were observed with a scanning electron microscope (SEM) (VEGA TS 5130 MM, Tescan, Czech Republic). To compare the density of the particles, a subsample of more than 50 particles were randomly selected from each particle sample. Assumed as spheres, their diameters were measured with sieves or the micrometer and the average diameter was calculated. The

total mass of the particles was weighed and the average mass was calculated. The density was then calculated by dividing the average mass to the average volume. Each density measurement was repeated at least three times and the standard deviation was within 5%. The density measured in this way is the envelope density: the ratio of the mass of a particle to the sum of the volume of: the solids in each piece and the voids within each piece, that is, within close-fitting imaginary envelopes completely surrounding each piece (ASTM D3766 in Webb, 2001).

2.3 Wastewater and solutions

One type of synthetic wastewater and three types of real wastewater were used in this study. The synthetic wastewater was prepared by dissolving diammonium hydrogen phosphate ($(\text{NH}_4)_2\text{HPO}_4$, VWR, Belgium) and ammonium chloride (NH_4Cl , Merck, Germany) with deionized water. The $\text{PO}_4\text{-P}$ and $\text{NH}_4\text{-N}$ concentration of the synthetic wastewater was 135 mg/L and 610 mg/L respectively (N:P molar ratio=10) which were the typical concentrations of $\text{PO}_4\text{-P}$ and $\text{NH}_4\text{-N}$ in the digested sludge supernatant from the WWTP with EBPR based on a literature review (Kumashiro et al., 2001; Britton et al., 2007; Ferrest et al., 2008). The real wastewaters were the filtrate of the undigested excess sludge from LFKW, the settled UASB reactor effluent from the dairy company Campina AG Heilbronn and the pre-treated digested sludge filtrate from the Offenburg WWTP. Their characteristics are summarized in Table 1. The LFKW uses chemical precipitation to remove P and thus the P concentration in the sludge filtrate was small (2 mg/L). A certain amount of phosphoric acid (H_3PO_4 , ortho-phosphoric acid 85%, Merck, Germany) and NH_4Cl were added in the filtrate to increase the $\text{PO}_4\text{-P}$ and $\text{NH}_4\text{-N}$ concentrations to be comparable with those of the synthetic wastewater. Before adding the chemicals, the pH of the LFKW filtrate was reduced to smaller than 5.5 to avoid precipitation. The pH, $\text{PO}_4\text{-P}$ and $\text{NH}_4\text{-N}$ concentration of the LFKW filtrate was 3.6, 159 mg/L and 560 mg/L respectively after the chemicals were added. The industrial wastewater contained a low concentration of $\text{PO}_4\text{-P}$ (74 mg/L). But its COD and TSS concentration was 6 times and triple that of the LFKW filtrate respectively. The industrial wastewater was used in the experiment without any adjustment. The pre-treated sludge filtrate was taken from the Stuttgart Process pilot plant located in the Offenburg WWTP. The pre-treatment included adding sulfuric acid (H_2SO_4) to the digested sludge to a pH of 4-5 to dissolve the P into the solution, and then separating the solution from the sludge with a chamber press filter with the aid of flocculants. The pre-treated sludge filtrate had very high concentrations of $\text{PO}_4\text{-P}$ (453 mg/L), $\text{NH}_4\text{-N}$ (1488 mg/L) and metal ions. To prevent the competition of the metal ions with Mg for $\text{PO}_4\text{-P}$, 150 mL citric acid was added in every 50 L pre-treated sludge filtrate to complex the metal ions (Preyl, oral communication). After citric acid addition, the pre-treated sludge filtrate had the largest concentrations of TSS, TOC and COD which were about twice those of the industrial wastewater. The TP concentrations of the three wastewaters were close to their $\text{PO}_4\text{-P}$ concentrations, i.e. almost all of the P was in dissolved form in the three wastewaters. The N:P and Mg:P molar ratio of the three real wastewaters was 7.3-10.4 and 0.2-0.4 respectively. Therefore, the $\text{NH}_4\text{-N}$ was in large excess with respect to $\text{PO}_4\text{-P}$ and external Mg sources needed to be added.

The external Mg source was supplied with the Mg solution which was made by dissolving magnesium chloride hexahydrate ($\text{MgCl}_2 \cdot 6\text{H}_2\text{O}$, Merck, Germany) with deionized water in all of the experiments except that with the pre-treated sludge filtrate, where solid magnesium oxide (MgO) or $\text{MgCl}_2 \cdot 6\text{H}_2\text{O}$ was added directly in the filtrate. The Mg:P molar ratio of all the experiments increased to 1.1-1.4 after the external Mg sources were added. 1 M NaOH solution made by dissolving NaOH pellets (Merck, Germany) with deionized water were used in the experiments.

Table 1: Characteristics of the three types of real wastewater used in this study

	LFKW filtrate	Industrial WW	Pre-treated sludge filtrate	
pH	3.6 ¹	7.1	3.6 ²	
COD	mg/L	321	1775	3008 ²
TSS	mg/L	163	452	694
TOC	mg/L	/	481	1184 ²
TP	mg/L	158 ¹	75	453
PO ₄ -P	mg/L	159 ¹	74	453
NH ₄ -N	mg/L	560 ¹	347	1488
NO ₂ -N	mg/L	/	<0.015	0.02
NO ₃ -N	mg/L	/	0.4	2.0
Cl ⁻	mg/L	/	115	161
SO ₄ ²⁻	mg/L	/	11	7660
Al	mg/L	1.4	0.3	0.5
Ca	mg/L	100	25	699
Fe	mg/L	0.4	0.8	58
Mg	mg/L	24	20	147
N:P		7.8	10.4	7.3
Mg:P		0.2	0.3	0.4

1- After pH and concentration adjustment

2- After citric acid and Mg source addition

2.4 Operational conditions

The operational conditions of the experiments are shown in Table 2. Altogether, five continuous struvite crystallization experiments (S1-S5) were carried out with the synthetic wastewater, among which four (S1-S4-2) were with the old reactor. Three additional continuous struvite crystallization experiments were carried out with the three types of real wastewater. The experiment with the LFKW filtrate was with the old reactor and the other two with the new reactor. The aim of S1 to S4-2 was to examine the influence of the operational conditions on the process efficiency and the product quality. Thus, except the operational conditions, the others were kept the same in the four experiments. The tested operational conditions included: the operational pH (pH_{op} , 7.4, 7.6, 7.8, 8.5 and 8.6), seed size (0.250-0.355 mm, 1.0-1.4 mm and 1.4-2.0 mm), seed amount (10 g, 15 g and 127 g), hydraulic retention time (HRT, 60 min and 109 min), recirculation flow rate (Q_{rec} , 400-1630 mL/min) and the experiment duration (18-35 d). Experiment 4 was divided into S4-1 and S4-2 with

different pH_{op} and Q_{rec} . The operational conditions of S5 were the same as S1 except for the slightly larger flow rates of the feed wastewater (Q_{ww}) and the Mg solution (Q_{Mg}). The aim of S5 was to verify the improvement of the product quality with the new reactor. Due to the different characteristics of the three types of real wastewater, the operational conditions of the three experiments with real wastewater varied. The industrial wastewater had a low PO_4 -P concentration. Thus, a very high pH_{op} (8.4) was used to reach a satisfactory PO_4 -P removal. Contrarily, the pre-treated sludge filtrate had a very high PO_4 -P concentration and the HRT was extended to 314 min to obtain a moderate supersaturation degree.

Table 2: Operational conditions of the experiments

Exp.	pH_{op}	Seed size mm	Seed amount g	HRT min	Q_{ww} mL/min	Q_{Mg} mL/min	Q_{rec} mL/min	Duration d
S1	7.6	0.250-0.355	10	109	27.6	2.8	400-1630	35
S2	7.4	0.250-0.355	10	109	27.6	2.8	1290, 1630	27
S3	8.5	0.250-0.355	5	109	27.6	2.8	740-1630	18
		1.0-1.4	5					
		0.250-0.355 sand	5					
S4-1	8.6	1.4-2.0	127	60	49.6	5.1	1700-2280	21
S4-2	7.8						770-1980	21
S5	7.6	0.250-0.355	10	104	29.0	3.2	400-1630	35
LFKW	7.6, 7.8	0.250-0.355	10	64	46.5	5.3	560-1930	41
Ind.	8.4	1.4-2.0	40	77	44.6	4.1	1600	21
Pre.	7.6	1.4-2.0	30	314	12.0	/	1600	35
		>3.15 Crushed frag.	4 6					

2.5 Definition of parameters

The process efficiency in this study included: the P recovery rate (%) which was the mass percentage of the P contained in the harvested product to the total P fed into the reactor during the experiment (Equation 2), the production rate (g/d) which was the mass the harvested product divided by the experiment duration (Equation 3), and the NaOH consumption amount ($NaOH_{con}$, g/d) which was the mass of solid NaOH consumed per day (Equation 4). The product quality was indicated by the product size, purity, envelope density, compactness and strength. The daily removal ratios of PO_4 -P, NH_4 -N and Mg (PO_4 -P_{rem}, NH_4 -N_{rem} and Mg_{rem}) were calculated with Equation 5-7.

$$P \text{ recovery rate} = \frac{M_{Pr.} \cdot TP\%}{\sum (TP_f \cdot Q_{N/P} \cdot 60 \cdot 24 / 1000000)} \quad \text{Equation 2}$$

$$\text{Production rate} = \frac{M_{Pr.}}{T} \quad \text{Equation 3}$$

$$NaOH_{con} = (M_S - M_E) \cdot C_{NaOH} \quad \text{Equation 4}$$

$$(PO_4 - P)_{rem} = \frac{(PO_4 - P)_f \cdot Q_{N/P} - (PO_4 - P)_e \cdot (Q_{N/P} + Q_{Mg})}{(PO_4 - P)_f \cdot Q_{N/P}} \quad \text{Equation 5}$$

$$(NH_4 - N)_{rem} = \frac{(NH_4 - N)_f \cdot Q_{N/P} - (NH_4 - N)_e \cdot (Q_{N/P} + Q_{Mg})}{(NH_4 - N)_f \cdot Q_{N/P}} \quad \text{Equation 6}$$

$$Mg_{rem} = \frac{Mg_f \cdot Q_{Mg} - Mg_e \cdot (Q_{N/P} + Q_{Mg})}{Mg_f \cdot Q_{Mg}} \quad \text{Equation 7}$$

- where - M_{Pr} . is the mass of the total harvested product, g;
- TP% is the TP content of the product, %;
 - TP_f , PO_4-P_f , NH_4-N_f and Mg_f are the daily feed concentrations of TP and the three ions, mg/L;
 - $Q_{N/P}$ and Q_{Mg} are the flow rates of the feed wastewater and Mg solution, mL/min;
 - T is the experiment duration, d;
 - M_S and M_E are the start and end mass of the NaOH solution bottle at every 24 h, g;
 - C_{NaOH} is the mass concentration of the NaOH solution, %;
 - PO_4-P_e , NH_4-N_e and Mg_e are the daily effluent concentrations of the three ions, mg/L;

3 Results and discussion

3.1 Influences of the operational conditions on the process efficiency

Figure 2 shows the relationship between the process efficiency, the removal ratios of PO_4-P , NH_4-N and Mg and the in-reactor solution pH (pH_{ir}) in the four experiments with synthetic wastewater and the old reactor. Except the P recovery rate and production rate, the others were the averages of the daily values in each experiment. It can be seen that the P recovery rates of the four experiments increased from 73.8% to 94.1% when the average pH_{ir} increased from 7.40 to 8.50. It was because the solubility of struvite decreases with the increasing pH in the tested pH range. Under a higher pH_{ir} , less of the feed PO_4-P , NH_4-N and Mg ions could remain dissolved in the solution. Therefore, more of them crystallized out of the solution as struvite crystals and were recovered. Due to the same reason, the average removal ratios of the three ions increased with the increasing average pH_{ir} . It is noticeable that the P recovery rate was 3-5% lower than the average PO_4-P_{rem} in the experiments except S4 (average $pH_{ir}=8.11$), meaning that some of the crystallized crystals were not harvested but lost as fine crystals with the effluent or lost during the harvesting and drying process. In the first 21 d of S4 (S4-1), a lot of fine crystals were generated in the reactor and were lost with the effluent. Due to this severe fines problem, the P recovery rate of S4 was 12% lower than the PO_4-P_{rem} and it was below the trend line of the other three data points in Figure 2.

The production rate was calculated based on the product quantity in this study (Equation 3). Theoretically, the production rate of a crystallizer was the quantity of the formed crystals which depended on the feed concentrations, feed flow rates and crystallization rate minus the losses. The feed concentrations of S1 to S4 were the same and thus the production rate of them depended on the feed flow rates, the crystallization rate which could be indicated by the $PO_4\text{-}P_{rem}$, and the losses. The production rate of S1 to S3 increased from 29.9 g/d to 41.0 g/d when the average pH_{ir} increased from 7.40 to 8.50 because the $PO_4\text{-}P_{rem}$ increased with the increasing pH_{ir} while their feed flow rates were the same. The production rate of S4 was 68.7 g/d. It was the largest among the four experiments because the feed flow rates and $PO_4\text{-}P_{rem}$ were the largest in S4.

Theoretically, the average $NaOH_{con}$ should also increase with the increasing average pH_{ir} , i.e. more NaOH is needed to keep a higher pH_{ir} . This was true for S1 to S3: the average $NaOH_{con}$ increased linearly with the average pH_{ir} ($R^2=0.9993$). However, the average $NaOH_{con}$ of S4 (average pH_{ir} 8.11) was much higher: it was more than triple those of S1 and S2 (average $pH_{ir}=7.55$ and 7.40 respectively) and even 57% higher than that of S3 whose average pH_{ir} (8.55) was actually higher. The high $NaOH_{con}$ of S4 was speculated to be caused by the using of the external clarifier which was not used in any other experiment. To settle the flushed out large number of fine crystals, the effluent collection tank was used as an external clarifier from the 10th day on in S4, and the supernatant of the external clarifier was recirculated into the reactor. The daily $NaOH_{con}$ increased obviously after the using of the external clarifier. One possible explanation is that the pH of the solution stored in the external clarifier dropped slightly during the storage due to CO_2 absorption or further struvite crystallization reaction. Thus, more NaOH solution was consumed to increase the pH of the recirculated solution from the external clarifier to pH_{op} .

Since the process efficiency of S1 to S4 depended largely on the pH_{ir} as shown above, the other operational parameters including the HRT, seed size, seed amount, recirculation flow rate and experiment duration had minor influence on the process efficiency except that the HRT (feed flow rates) and feed concentrations affected the production rate besides the pH_{ir} .

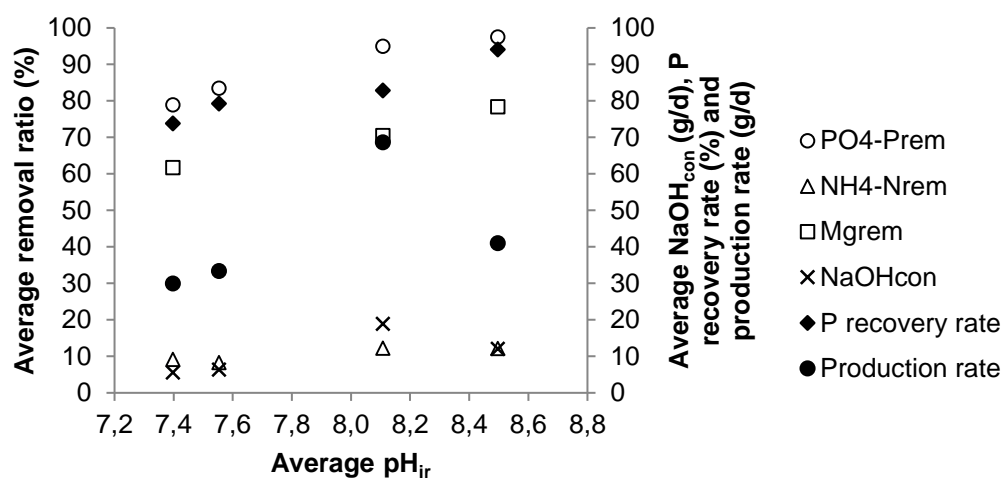


Figure 2: Relationships between $PO_4\text{-}P_{rem}$, $NH_4\text{-}N_{rem}$, Mg_{rem} , $NaOH_{con}$, P recovery rate, production rate and pH_{ir} in S1 to S4

3.2 Influences of the operational conditions on the product quality

3.2.1 Size

The sizes of the seeds and the largest particles harvested during and at the end of each experiment are shown in Figure 3 over the experiment duration. It has to be mentioned that particles of smaller sizes were also harvested during and at the end of each experiment, but they were not considered here because it was not clear how long the smaller particles had grown in the reactor (the retention time), while it was certain that the retention time of the largest particles equaled to the experiment duration before they were harvested. Particles larger than 3.0 mm were produced in each experiment except in S2. The largest particles (3.5-4.0 mm) were produced in S1 and S4-2 with the longest experiment duration which was 35 d and 42 d respectively. The particle size increased with the experiment duration in each experiment, indicating that if the experiment duration was extended, bigger particles could be produced. However, due to the restriction of the available Q_{rec} and the reactor scale, a maximum particle size would exist. Most of the experiments had larger crystal growth rates in the first week than in the rest duration, especially in S1 where the particle size jumped from 0.3 mm to 1.7 mm after the first week. This could be owing to the small size of the seeds which provided plenteous surface area to integrate new crystals and thus the growth rate was large.

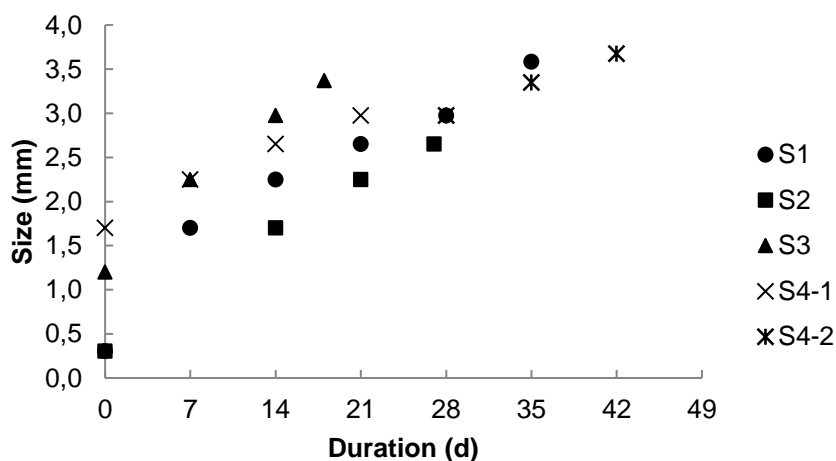


Figure 3: Size of the seeds and the largest particles harvested in S1 to S4

3.2.2 Compactness, hardness and envelope density

Through XRD and composition analysis, it was confirmed that the largest particles harvested at the end of S1 to S4 were pure struvite. Their compactness was revealed by their morphologies which are shown in Figure 4. The particles from all of the four experiments were crystal aggregates which were spherical in shape except those from S4-1. However, the surface morphologies of the particles from different experiments varied significantly. The particles from S1 were the most compact and strongest. They had smooth compact surfaces with small fissures. The surfaces of the particles from S2 and S4-2 were composed of tips of brick-like single crystals. Those crystals were disordered and compacted in the particles from S4-2, while those in the particles from S2 were oriented radially and were less compact. The surfaces of the particles from S3 consisted also of single struvite crystals, but these crystals

were smaller than those from S2 and S4-2. The particles from S4-1 were irregular in shape, and the surface was a porous accumulation of tiny fluffy powders which were very brittle. Those particles from S4-1 were the least compact and with the least strength. Figure 4, 1C shows the cross section of the one of the largest particles from S1. It reveals that the particle was composed of a compact outer surface layer made up of numerous tiny crystals with the size of several μm and an inner core of crystal aggregates made up of radially arranged big crystals. The particles from S2, S3 and S4-2 were composed of only big crystals and no compact small-crystal layers were observed. It seemed that the compact small-crystal layer increased the compactness and strength of the particles from S1.

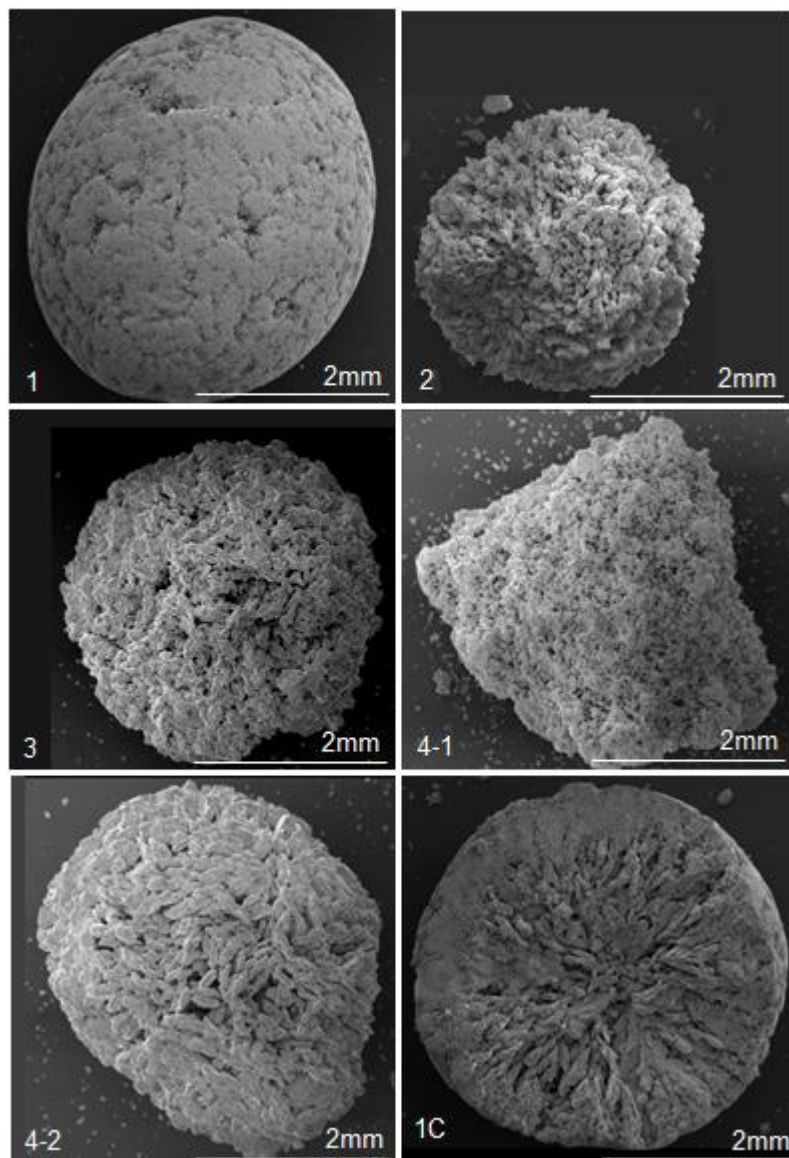


Figure 4: SEM images of the largest particles harvested at the end of S1 to S4. 1: >3.15 mm particle from S1; 2: 2.5-2.8 mm particle from S2; 3: >3.15 mm particle from S3; 4-1: 2.8-3.15 mm particle from S4-1; 4-2: >3.15 mm particle from S4-2; 1C: cross section of the >3.15 mm particle from S1. The scale was adjusted to be the same.

The envelope density of the particles (Figure 5) correlated well with their morphology: the more compact the particles, the larger the envelope density. The largest particles from S1

had the largest envelope density which was 1100 kg/m^3 . Those from S3 and S4-2 followed with the envelope density of 1000 kg/m^3 . The third ones were those from S2 with the envelope density of 870 kg/m^3 . The envelope density of the largest particles from S4-1 was the smallest (800 kg/m^3). By dividing the envelope density by the true density of struvite (1700 kg/m^3), it could be conducted that the porosity of the harvested particles was between 35% and 53%.

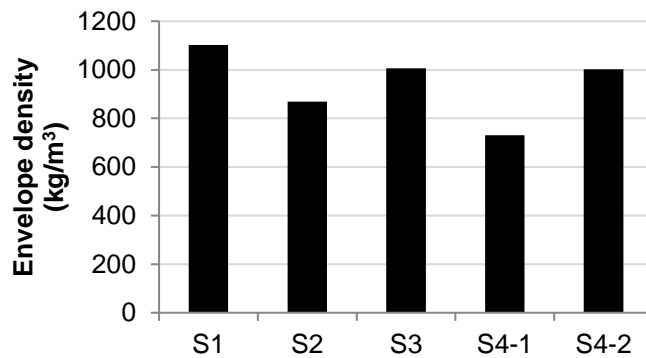


Figure 5: Envelope density of the largest particles harvested at the end of S1 to S4

The different morphologies, compactness and strength of the particles derived from the different operational conditions of the experiments. Research has shown that the size of single struvite crystal was related to the supersaturation degree. When the supersaturation degree exceeds the metastable limit, primary nucleation predominates and generates massive fine crystals (von Münch and Barr, 2001; Le Corre et al., 2007). In S4-1, the pH_{ir} (8.55) and the flow rates of the wastewater and Mg solution were the highest among all the experiments, leading to the highest supersaturation degree and the formation of the fine crystals. They were attached loosely on the surface of the large seed particles (1.4-2.0 mm), forming the brittle crystal aggregates with the least compactness and strength. Some of the tiny crystals were flushed out of the reactor with the effluent, causing the fines problem mentioned in section 3-1. In S3, the pH_{ir} (8.50) was also high, but the flow rates of the wastewater and Mg solution were smaller and the small seeds (0.250-0.355 mm) had larger surface area for crystal growth which consumed some of the dissolved ions and reduced the supersaturation degree. Thus, the single crystals of the particles from S3 were larger than those from S4-1 but smaller than those from S2 and S4-2 which had smaller pH_{ir} values and smaller supersaturation degree. The compact small-crystal layer formed only on the surfaces of the particles from S1. The formation mechanism will be discussed in section 3.5. The obstructed particle fluidization in S2, the short experiment duration of S3, and the small seed size and short duration of S4-2 prevented the formation of the compact small-crystal layers.

In conclusion, the particle size increased with the experiment duration in each experiment, and the particle compactness, strength and envelope density were influenced by all of the operational parameters including the pH, feed flow rates (HRT), seed size, recirculation flow rate and experiment duration. Since the particle size was related to the compactness, it was also influence by all of the parameters besides the experiment duration.

3.3 Improvement of the product quality with the new reactor

The largest particles harvested at the end of S5 which was carried out under the same operational conditions as S1 but with the new reactor reached an average size of 4.1 cm and an envelope density of 1390 kg/m³. Both of the size and the envelope density of these particles were larger than the particles from S1. Moreover, the particles from the new reactor had improved compactness. Their surfaces were very smooth and without any fissures (Figure 6, left). The inside single crystals were compactly arranged and the compactness of the particle increased gradually from the center to the surface (Figure 6, right). The thickness of the compact small-crystal layer of these particles was approximately 0.3 mm larger than those from S1. The missing part on the top of the cross section (Figure 6, right) was because this part was cut off when preparing the cross section. Actually, the particle was so hard that it was very difficult to cut it with a razor blade. Thus, the new reactor with an extended 2.2 cm section improved the size, envelope density, compactness and strength of the produced largest particles.

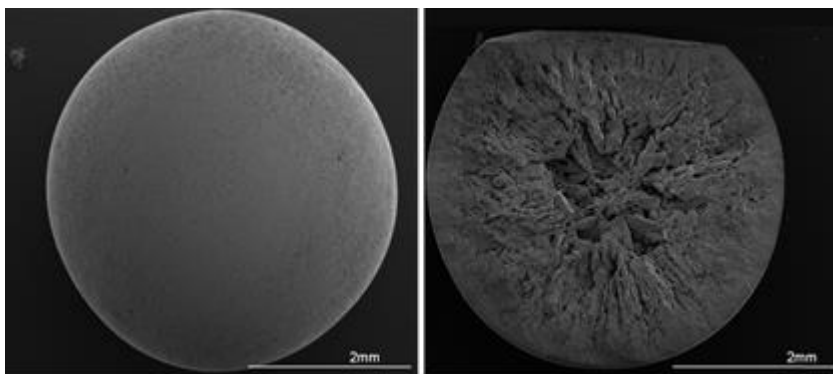


Figure 6: SEM images of the surface (left) and cross section of the largest particles from S5

3.4 Process efficiency and product quality of the experiments with the three types of real wastewater

3.4.1 Process efficiency

The process efficiencies and $PO_4\text{-}P_{\text{rem}}$ of the experiments with the three types of real wastewater are shown in Table 3. The P recovery rate of the experiment with the LFKW filtrate was 64.5%. It was around 15% lower than that of S1 with approximately the same pH_{op} . The reason included that: 1) the real wastewater had a higher ionic strength than the synthetic wastewater and thus the activities of the $PO_4\text{-}P$, $NH_4\text{-}N$ and Mg ions decreased, resulting in a lower crystallization rate; 2) more fine crystals were lost with the effluent by combing with the suspended solids contained in the real wastewater; 3) the harvested product from the experiment with real wastewater had a lower P content due to the presence of impurities. The P recovery rate of the experiment with the pre-treated sludge filtrate was 61.1% although the average $PO_4\text{-}P_{\text{rem}}$ was 95.6% because large amount of P was lost with the effluent. In the experiment with the industrial wastewater, the $PO_4\text{-}P_{\text{rem}}$ was not so high (77.3%) and the loss of P as fine crystals was large ($PO_4\text{-}P_{\text{rem}}\text{-}TP_{\text{rem}}=23.5\%$). Consequently, the P recovery rate of the experiment with the industrial wastewater (57.1%) was the lowest among the three experiments.

As mentioned in section 3.1, the production rate depended on the feed flow rates, feed concentration, crystallization rate ($PO_4\text{-}P_{\text{rem}}$) and the loss. The feed flow rates in the experiment with the LFKW filtrate were around twice those in S1 and their feed concentrations were close. Therefore, the production rate of the experiment with the LFKW filtrate (55.9 g/d) was higher than that of S1 although the $PO_4\text{-}P_{\text{rem}}$ was slightly smaller. Contrarily, the feed flow rate in the experiment with the pre-treated sludge filtrate was only one fourth of that in the experiment with the LFKW filtrate. Moreover, many tiny crystals were lost with the effluent. Thus, although the pre-treated sludge filtrate had a much higher $PO_4\text{-}P$ concentration and around 96% of them crystallized in the reactor, the production rate (39.6 g/d) was smaller. The production rate in the experiment with the industrial wastewater (22.1 g/d) was the smallest because the feed $PO_4\text{-}P$ concentration was the smallest among the three experiments, the $PO_4\text{-}P_{\text{rem}}$ and feed flow rates were close to those of the experiment with the LFKW filtrate, and lots of fine crystals were lost with the effluent.

The $NaOH_{\text{con}}$ of the three experiments ranged between 24.8 g/d and 48.1 g/d. It was the smallest in the experiment with the industrial wastewater because the industrial wastewater had a much higher pH (7.1) than the other two feed wastewaters. The adjusted pH of the feed LFKW filtrate and pre-treated sludge filtrate were the same (3.6) and their pH_{op} were close. However, more NaOH was consumed in the experiment with the pre-treated sludge filtrate. The explanation could be that the pre-treated sludge filtrate had a much higher concentration of organic substances, i.e. the COD concentration of the pre-treated sludge filtrate was more than 9 times that of the LFKW filtrate. The organic substances increased the buffering capacity of the pre-treated sludge filtrate and thus more NaOH was consumed.

Table 3: P recovery rate, production rate, $NaOH_{\text{con}}$ and $PO_4\text{-}P_{\text{rem}}$ in the experiments with the three types of real wastewater

	P recovery rate %	Production rate g/d	$NaOH_{\text{con}}$ g/d	$PO_4\text{-}P_{\text{rem}}$ %
LFKW filtrate	64.5	55.9	35.7	74.9
Industrial WW	57.1	22.1	24.8	77.3
Pre-treated sludge filtrate	61.1	39.6	48.1	95.6

3.4.2 Product quality

Photos of the largest particles harvested at the end of the experiments with the three types of real wastewater are shown in Figure 7 and their qualities are shown in Table 4. The particles from the experiment with the LFKW filtrate were broken ellipsoids with the average size of 3.9 mm. The crystal aggregates grown from the small struvite seeds broke in the reactor during the experiment with the LFKW filtrate. Thus, the finally harvested particles were broken and the density was not measured. To avoid this, large struvite particles were used as seeds in the other two experiments and the products were spherical pellets with the average diameter of 2.3 mm and 3.4 mm respectively from the experiment with the industrial wastewater and pre-treated sludge filtrate. The industrial wastewater had a low $PO_4\text{-}P$ concentration and the experiment duration was short. Hence the product size was smaller.

The x-ray diffractograms of those largest particles from all of the three experiments matched well with the standard struvite diffractogram and no peaks of other crystals were found in any of them. However, their TP contents (12.1-12.2%) were smaller than that of pure struvite. Therefore, the particles were composed of struvite and some amorphous impurities which could be suspended solids from the real wastewaters and amorphous precipitates formed in the reactor. The purities of these particles calculated by dividing their TP or TKN content to that of struvite ranged 96% to 97%.



Figure 7: : Photos of the largest particles harvested at the end of the experiment with the LFKW filtrate (left), the industrial wastewater (middle) and the pre-treated sludge filtrate (right). The magnification of the photos was different.

Table 4: Average size, envelope density, elemental contents and purity of the largest particles harvested at the end of the experiments with the three types of real wastewater

	Average size mm	Envelope density kg/m ³	TP %	TKN %	Purity %
LFKW filtrate	3.9	/	12.2	5.7	96.7
Industrial WW	2.3	1220	12.1	5.7	95.9
Pre-treated sludge filtrate	3.4	1574	12.1	5.6	95.9
Struvite			12.6	5.7	

The envelope density of the largest particles from the experiment with the pre-treated sludge filtrate reached 1574 kg/m³. It was the highest among the particles produced from all of the experiments carried out in this study because these particles had the thickest compact small-crystal layer (Figure 8). The crystal aggregate in the center of the cross section was the 1.4-2.0 mm seed particle. Compact small-crystal layers formed adjacent to the surface of the seed particle and grew layer by layer. The colors of different layers varied (Figure 8, right) because the in-reactor solution conditions changed during the experiment. These particles were very strong and could not be crushed with the fingers. Compact small-crystal layers formed also adjacent to the seed particles in the experiment with the industrial wastewater. However, these layers were very thin. Thus, the finally harvested particles from the experiment with the industrial wastewater had a smaller density (1220 kg/m³) and were not so strong.

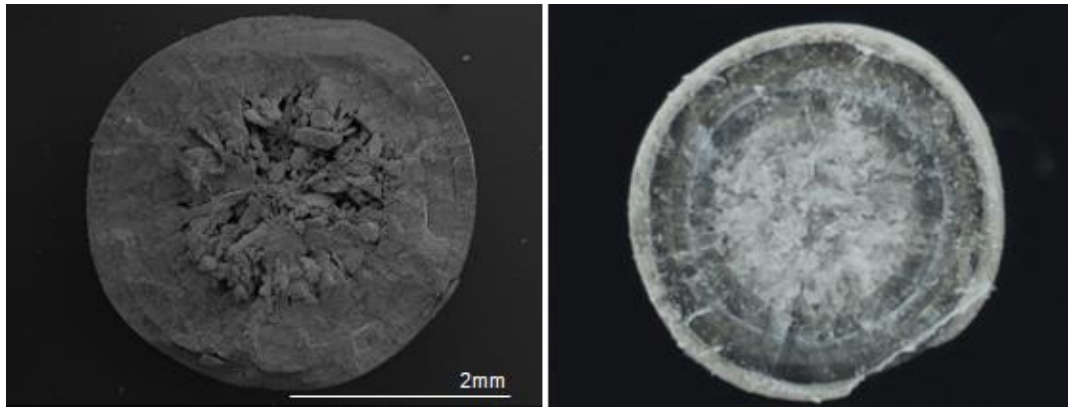


Figure 8: A SEM image (left) and a photo (right) of the cross section of one of the largest particles harvested at the end of the experiment with the pre-treated sludge filtrate.

3.5 Formation process of the large compact struvite particles

The formation process of the compact particles in S5 was revealed by the surface morphologies of the particles harvested during this experiment (Figure 9). The 0.250-0.355 mm seeds grew to 1.4-2.0 mm crystal aggregates after one week (Figure 9, 1). The particles kept growing in size by integrating new crystals on the surface; but the size of the integrated single crystals decreased and the voids between the single crystals diminished with time (Figure 9, 2-4). Eventually, the single crystals became so small that the voids between them almost disappeared, and the surface looked like a whole block (Figure 6, left).

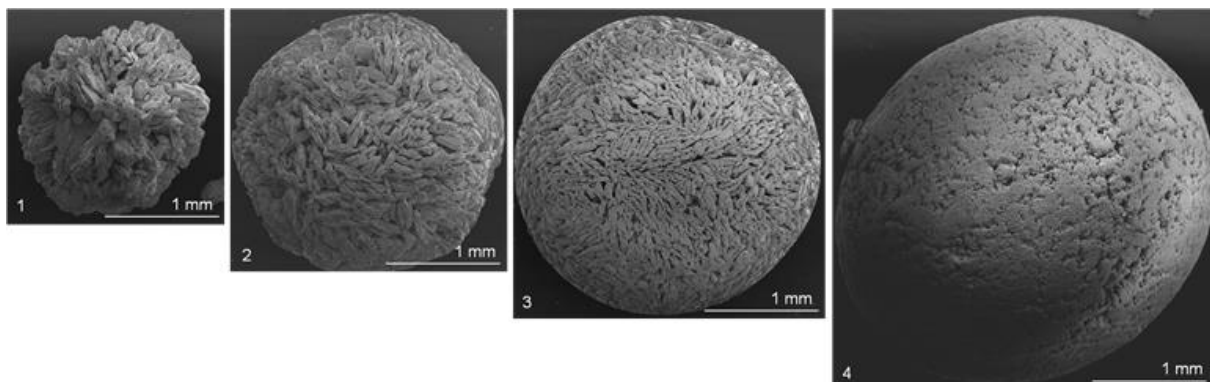


Figure 9: SEM images of the surfaces of the largest particles harvested during S5. 1: 1.4-2.0 mm particle harvested on the day 7; 2: 2.0-2.5 mm particle harvested on the day 12; 3: 2.0-2.5 mm particle harvested on the day 14; 4: 2.8-3.15 mm particle harvested on the day 21. The scales of these images were adjusted to the same.

The size decrease of the surface crystals was possibly related to the steady increase of the recirculation flow rate from 400 mL/min to 1630 mL/min during S5. Pohlisch and Mersmann (1988) demonstrated in their KNO_3 crystallization experiments with a draft tube reactor equipped with a stirrer that the mean particle size decreased with the increasing attrition rate which increased with the increasing velocity. In the experimental FBR, the steadily increased recirculation flow rate increased the upflow velocity in the reactor. Thus, the attrition rate increased and the crystal size decreased.

In the experiments with the industrial wastewater and pre-treated sludge filtrate, the highest recirculation flow rate (1600 mL/min) was applied at the beginning of the experiment, and the 1.4-2.0 mm struvite particles were added as seeds. Some of the seed particles fluidized in the bottom 2.2 cm section where the upflow velocity and thus the attrition rate was the highest. Thus, crystals of very small size formed. They were integrated to the surface of the seed particles, building the compact small-crystal layer.

4 Conclusion and outlook

Based on the experimental results, the following conclusions can be drawn from this study:

- Among the tested operational parameters, pH played a decisive role in the process efficiency. The P recovery rate, production rate and NaOH consumption increased with the increasing pH.
- Contrarily, all of the operation pH, HRT, seed size, recirculation flow rate and experiment duration influenced the size, morphology, envelope density, compactness and strength of the produced particles. High pH (8.55), short HRT (60 min) and large seeds (1.4-2.0 mm) led to the formation of brittle particles which were irregular in shape, loose, with the lowest envelope density and broke very easily. The size of the in-reactor particles increased with the experiment duration.
- The new reactor with an extended 2.2 cm reaction section improved the size, envelope density, compactness and strength of the produced particles. The upflow velocity in this section with the recirculation flow rate of 1600 mL/min was about 420 cm/min, close to the value reported by Fattah (2010).
- When operating the struvite crystallization FBR with real wastewater, large (1.4-2.0 mm) struvite particles should be added as seeds instead of small (0.250-0.355 mm) struvite particles because the crystal aggregates grown from the small struvite seeds broke in the reactor.
- 2.0-4.0 mm compact spherical struvite pellets were successfully recovered from the industrial wastewater from the dairy company Campina AG Heilbronn and the pre-treated sludge filtrate from the Offenburg WWTP with chemical P removal. The purity of these particles was higher than 95%.

There were also limitations in this study which need further research. The most important one was that the mass percentage of the large compact particles in the entire product was too small. For example, in the experiment with the pre-treated sludge filtrate, the larger than 3.15 mm particles accounted for only 11% of the entire product while 77% of the entire product were smaller than 1 mm. Improvement could possibly be accomplished by further optimizing the reactor design. One direction could be extending further the 2.2 cm section and shortening or even deleting the 4.2 cm section. Meanwhile, the diameter and height of the precipitation section might need to be extended since more small crystals would be brought up to the precipitation zone with the shortened or no 4.2 cm section. The determination of the exact heights of the 2.2 cm and 4.2 cm sections, and the appropriate

diameter and height of the precipitation section needs to consider the hydrodynamics of the reactor and the kinetics of struvite crystallization reaction.

Reference

- Britton A.T., Sacluti F. Oldham W.K., Mohammed A., Mavinic D.S. and Koch F.A. (2007). Value from waste-struvite recovery at the city of Edmonton's Gold Bar WWTP. *Proceedings of the Joint IWA/WEF Specialty Conference on "Wastewater Biosolids Sustainability"*, Moncton, N.B., June 24-27, 2007.
- Cordell D., Drangert J.O. and White S. (2009). The story of phosphorus: Global food security and food for thought. *Global Environmental Change*, 19, 292-305.
- Fattah K.P. (2010). *Development of control strategies for the operation of a struvite crystallization process*. PhD thesis, Department of Civil Engineering, University of British Columbia, Vancouver, Canada.
- Forrest A.L., Fattah K.P., Mavinic D.S. and Koch F.A. (2008). Optimizing struvite production for phosphate recovery in WWTP. *Journal of Environmental Engineering*, May 2008: 395-402.
- Günther F. (1996). Hampered effluent accumulation process: Phosphorus management and societal structure. *Ecological Economics*, 21, 159-174.
- Heffer and Prud'homme, IFA (2013). Fertilizer outlook 2013-2017. *81th IFA Annual Conference*, Chicago (USA), 20-22 May 2013.
- Kumashiro, K., Ishiwatari H, Nawamura Y (2001). A pilot plant study on using seawater as magnesium source for struvite precipitation. 1Water Quality Control Section, Construction Bureau, 96-3 Nishiminato-Mati, Kokurakita-Ku, Kitakyushu, 803-0801, Japan.
- Le Corre K. S., Valsami-Jones E., Hobbs P., Jefferson B. and Parsons S.A. (2007). Struvite crystallization and recovery using a stainless steel structure as a seed material. *Water Resource*, 41, 2449-2456.
- Le Corre K. S., Valsami-Jones E., Hobbs P., Jefferson B. and Parsons S. A. (2009). Phosphorus recovery from wastewater by struvite crystallization: A review. *Critical Reviews in Environmental Science and Technology*, 39, 433-477.
- Montag D.M. (2008). *Phosphorrückgewinnung bei der Abwasserreinigung–Entwicklung eines Verfahrens zur Integration in kommunale Kläranlagen*. Doctor thesis, Department of Civil Engineering, RWTH Aachen, Aachen, Germany.
- Piekema P. and Giesen A. (2001). Phosphate recovery by the crystallization process: Experience and developments. *Proceedings of 2nd International Conference on Recovery of Phosphates from Sewage and Animal Wastes*, Holland, NL, 12-13 March 2001.
- Pohlisch J. and Mersmann A. (1988). The influence of stress and attrition on crystal size distribution. *Chemical Engineering & Technology*, 11: 40-49.
- von Münch E. and Barr K. (2001). Controlled struvite crystallization for removing phosphorus from anaerobic digester sidestreams. *Water Research*, 35(1), 151-159.
- Webb P. A. (2001). Volume and density determinations for particle technologies. Micromeritics Instrument Corporation, Georgia, USA.
- Weideler A. (2010). Phosphorrückgewinnung aus kommunalem Klärschlamm als Magnesium-Ammonium Phosphat (MAP). *Stuttgarter Berichte zur Siedlungswasserwirtschaft*, Band 202.

24.09.2014

Pengfei Wang